Haptic Rendering and Human Stabilization in Presence of Structural Flexibility

Csaba Budai†, László L. Kovács‡ and József Kövecses§

Abstract

Unstable behaviour is a significant problem in many haptic applications. The sampled-data nature and time delays induce complex dynamic behaviours in such systems. Structural flexibility may further reduce the stable domain of operation. This is illustrated via the systematic modeling and analysis of an impedance type haptic device with typical design elements such as closed-loop mechanisms and cable/capstan drives. The role of the operator in the dynamics of these systems is also demonstrated. The present work provide stability analysis, experimental validation and derive conditions for the range of parameters in which the operator can significantly contribute to the stabilization of the system.

Representative Haptic Models

Impedance type *kinesthetic haptic* devices are usually multi-DoF mechanisms, that transfer forces to the human user to create the sense of physical interaction with a virtual environment. Usually, the haptic system consists of three main parts: the *haptic device*, the *virtual environment*, and the *human operator* (see Fig. 1).

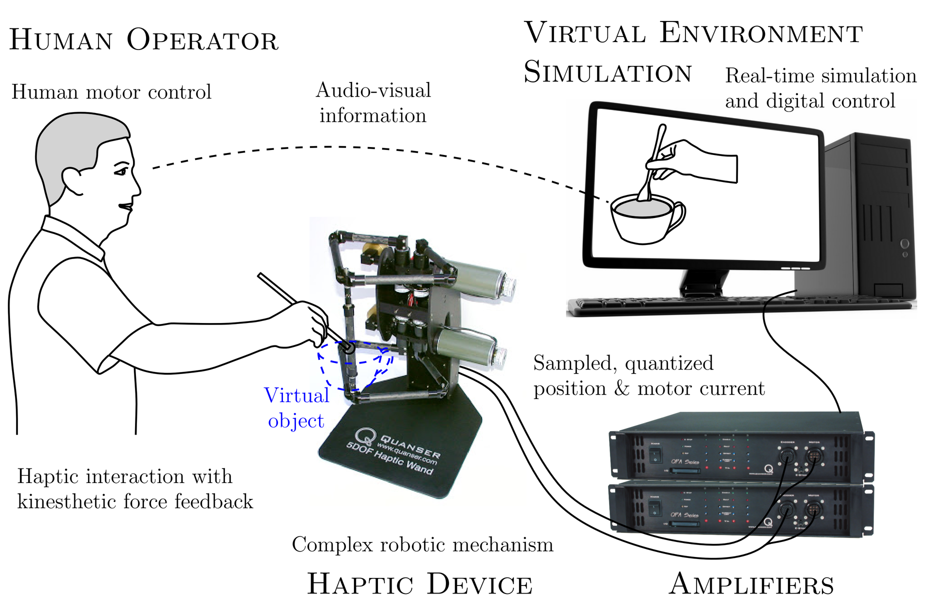

Figure 1: Haptic system sketch

Generally, the linearized dynamical model of a haptic system can be written in the form

$$\mathbf{M}\ddot{\mathbf{q}} = \mathbf{f}_h + \mathbf{f}_d + \mathbf{f}_k + \mathbf{f}_v \tag{1}$$

where $\mathbf{f}_h$ represents the force applied by the human operator, $\mathbf{f}_d$ and $\mathbf{f}_k$ comes from the dissipation and the structural flexibility. The force generated by the virtual environment is denoted by $\mathbf{f}_v$.

Mass orthogonal decomposition can be used to obtain fully decoupled and/or representative parametric models for analyses and design optimization. In the presence of structural flexibility one has to consider also that the application of the physical and virtual forces are not co-located.

As an example, a five-bar linkage based system with capstan drive is shown in Fig. 2, where structural flexibility mainly arises due to the bending of the motors' shafts and the torsional deformation of the driving arms.

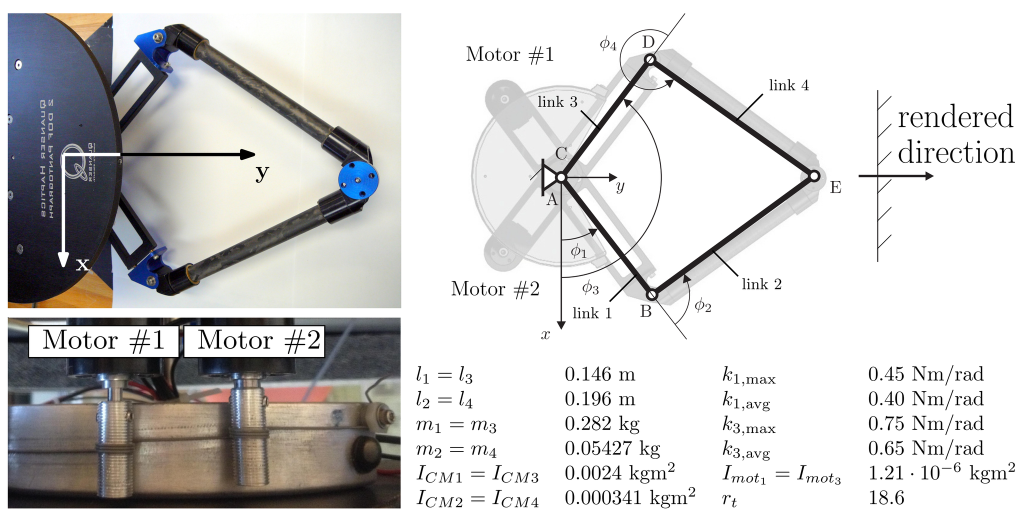

Figure 2: Experimental system with capstan drive

The haptic force generation in the rendered direction can parametrically be investigated by the structural model presented in Fig. 3.

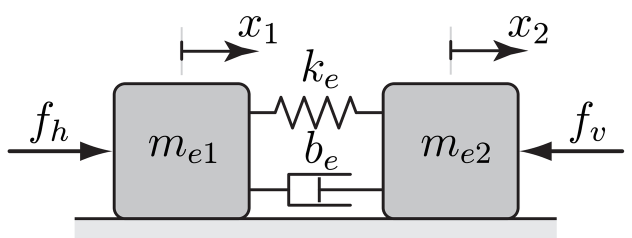

Figure 3: 2 DoF structural model in the rendered direction

The analytically derived equation of motion in the single rendered direction is

$$\begin{aligned} m_{e1}\ddot{x}_1 + k_e(x_1 - x_2) &= f_h + f_{d1} \\ m_{e2}\ddot{x}_2 + k_e(x_2 - x_1) &= f_v + f_{d2} \end{aligned} \tag{2}$$

where $m_{e1} = \left(\mathbf{A}_1\mathbf{M}^{-1}\mathbf{A}_1^{\mathrm{T}}\right)^{-1}$ and $m_{e2} = \left(\mathbf{A}_2\mathbf{M}^{-1}\mathbf{A}_2^{\mathrm{T}}\right)^{-1}$ are the effective masses, $k_e = \left(\mathbf{J}\mathbf{K}^{-1}\mathbf{J}^{\mathrm{T}}\right)^{-1}$ is the effective stiffness. Transformations $\mathbf{A}_1 = [\mathbf{J}\ \mathbf{0}]$ and $\mathbf{A}_2 = [\mathbf{0}\ \mathbf{J}]$ consider the different points of application for the physical and virtual forces, and $\mathbf{J}$ (in the present example) is the second row of the manipulator's Jacobian. In addition f_h is the human operator force, f_{d1} and f_{d2} are the dissipation forces, and f_v is the virtual interaction force. This force is typically expressed in the form

$$f_v = -k_p x_2(t_j) - k_d v_2(t_j)\,, \quad t \in [t_j, t_{j+1}) \tag{3}$$

where k_p is the virtual stiffness and k_d is the virtual damping, Δt is the sampling time, $t_j = j\Delta t$, and $v_2(t_j)$ is the estimated velocity from encoder position data.

When low virtual impedances are to be rendered, the flexible mode has usually little effect on the dynamics. The rigid body model in Fig. 4 with $m \approx m_{e1}$ approximates well the dynamic behaviour. In higher frequency ranges, mostly the flexible mode is excited. This is captured by the 1 DoF flexible model in Fig. 4.

Figure 4: Simplified 1 DoF rigid (left) and flexible (right) models

Stability Analysis and Dynamics Characterization

The stability of different models were investigated by considering backward difference approximation for the velocity term in Eq. (3). In each cases, discrete maps were derived to characterize the controlled dynamics of the given sampled data systems. The different stable domains are summarized in Fig. 5. Here the shaded area is a measure of the impedance range of the analysed haptic device. This measure can be approximated by the closed form expression (4) obtained with the 1 DoF flexible model without damping.

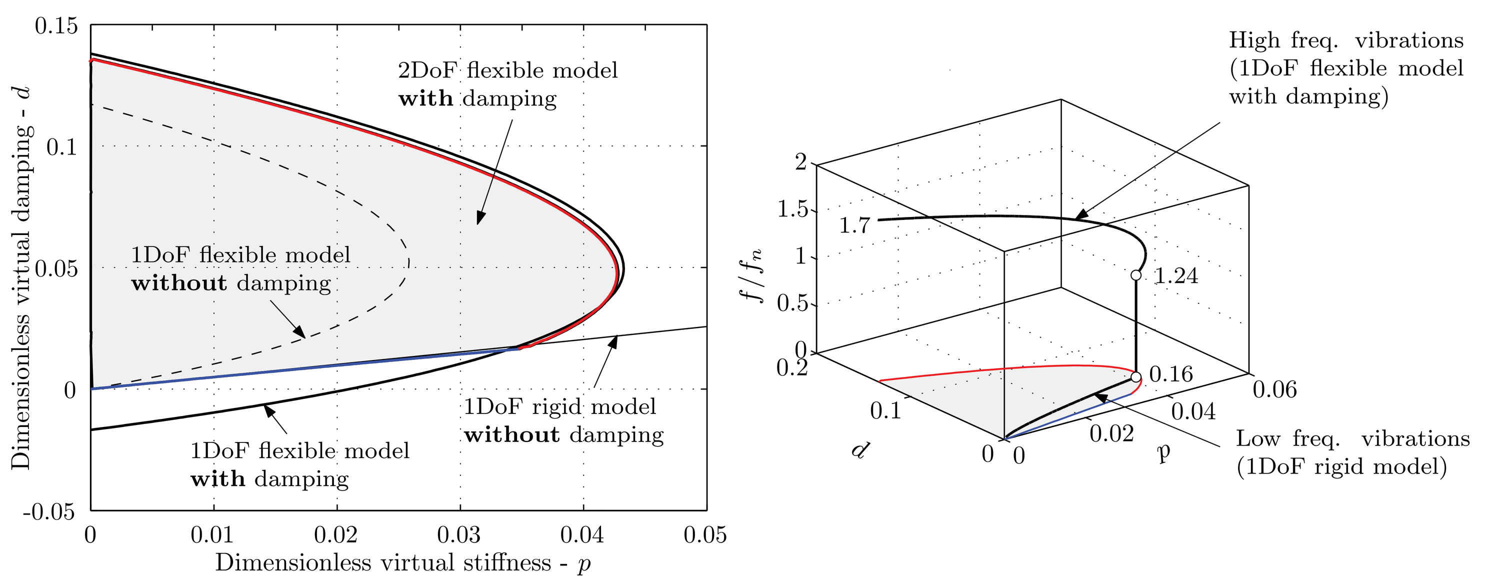

Figure 5: Stability and vibrations of different haptic models

$$w_A = \frac{m_{e2}^2}{\Delta t^3}\frac{\Omega_n^4}{\sin^4\frac{\Omega_n}{2}}\left(1 + 4\cos\Omega_n + \cos 2\Omega_n - 4\left(1+\cos\Omega_n\right)\ln\left(1+\cos\Omega_n\right)\right) \tag{4}$$

The analysis confirmed that the stable domain can be divided into two parts. For low impedances the system loses its stability with low frequency vibrations, while for higher impedance values the loss of stability occurs at higher frequencies. The calculated stability boundaries were verified by experiments. The observed sudden change in the vibration frequencies is explained by the frequency plots (e.g., $f/f_n - d$) along the stability limits.

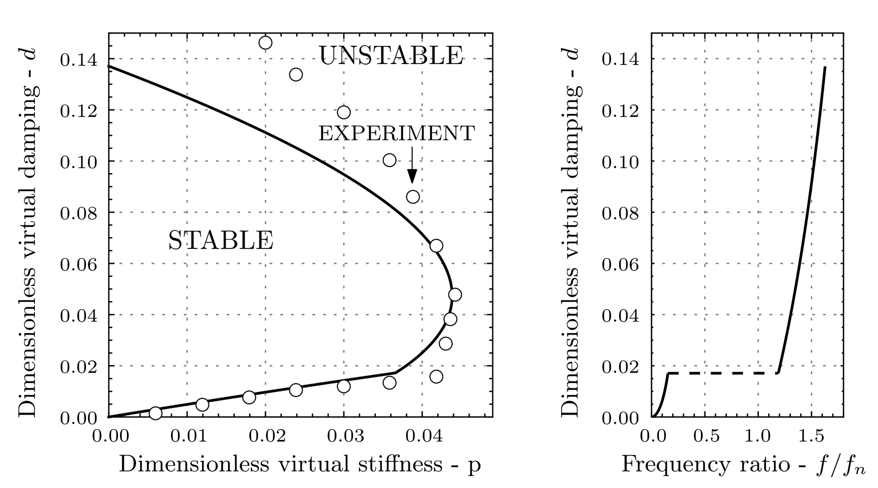

Figure 6: Experimental results w/o human operator

Human Effect on System's Stability

Without human operator, $f_h = 0$ in Eq. (2), the theoretical and experimental stability charts show a good agreement at lower virtual damping values (Fig. 6). Here, it was also observed that the human operator can actively compensate for instabilities. For larger virtual damping the difference is mainly because of the simple representation of physical dissipations in the model.

To qualitatively explain the operator's active contribution, here, we consider a delayed oscillator model which captures the dynamics of the haptic system at the loss of stability, and models the effect of the operator with delayed force feedback terms

$$\ddot{x}(t) + \frac{\kappa}{\tau^2}x(t) = -c\,\frac{\kappa}{\tau^2}x(t-\tau) - b\,\frac{\kappa}{\tau}\dot{x}(t-\tau) \tag{5}$$

In this equation $\kappa = (2\pi f)^2\tau^2$ with f referring to the dominant vibration frequency at the loss of stability (see Fig. 5 and 6), while c and b are the dimensionless proportional and differential force gains, and τ is the reflex delay. The resulting stability charts for different values of the dimensionless stiffness κ are presented in Fig. 7, where the area of the stable domain shows the ability of the human operator to compensate for the instabilities due to sampling effects.

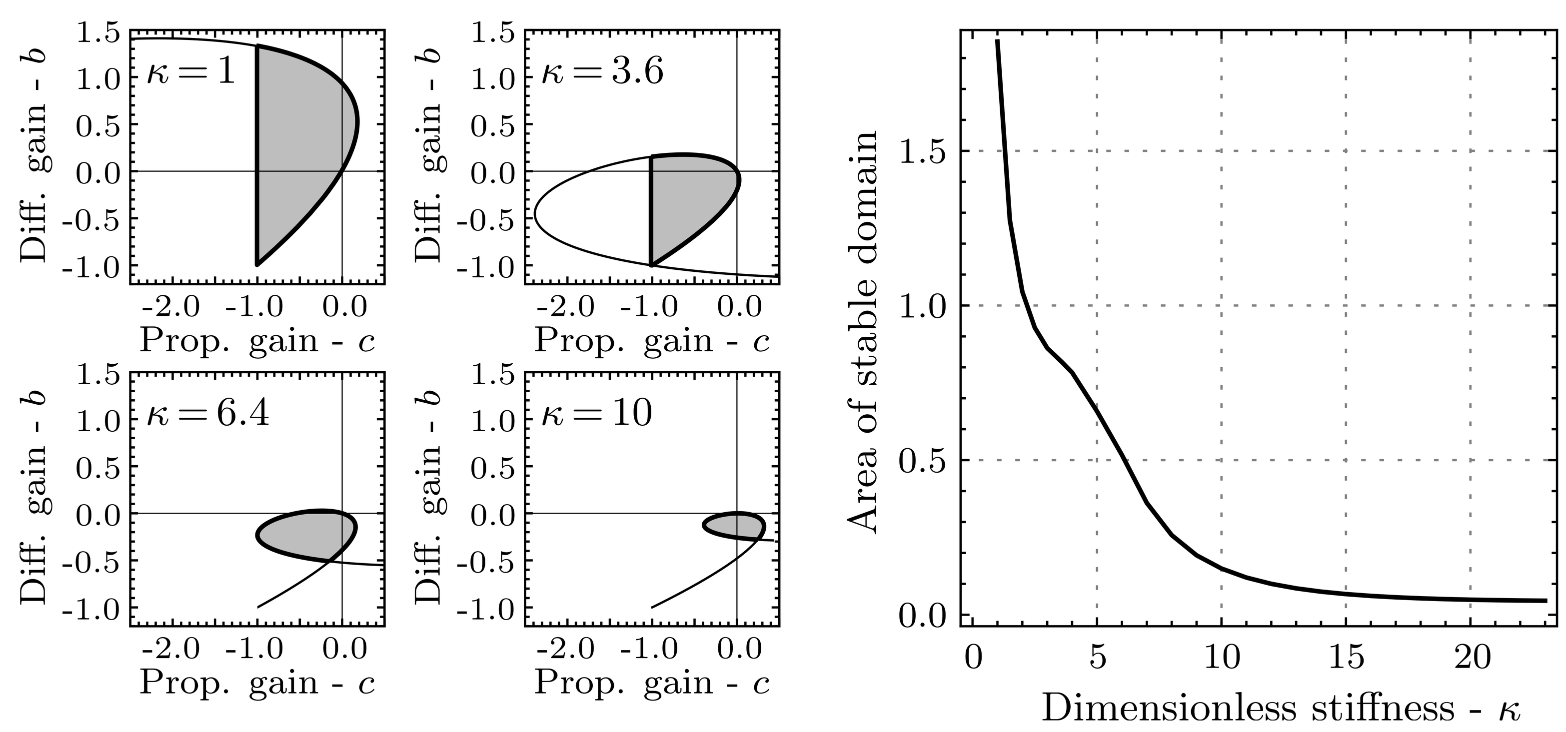

Figure 7: Compensation by human operator at the loss of stability

† Csaba Budai (budaicsaba@mogi.bme.hu), Department of Mechatronics, Optics and Mechanical Engineering Informatics, Budapest University of Technology and Economics, Budapest, Hungary

‡ László L. Kovács (kovacs@mm.bme.hu), MTA-BME Research Group on Dynamics of Machines and Vehicles, Budapest, Hungary

§ József Kövecses (jozsef.kovecses@mcgill.ca), Centre for Intelligent Machines, Department of Mechanical Engineering, McGill University, Montréal, Québec, Canada